Isotropic-nematic phase transition: Influence of intramolecular flexibility using a fused hard sphere model

Carl McBride, Carlos Vega, and Luis G. MacDowell*
Departamento de Química Física, Facultad de Ciencias Químicas, Universidad Complutense de Madrid, Ciudad Universitaria, 28040 Madrid, Spain

(Received 20 December 2000; published 14 June 2001)

The role of flexibility on the liquid crystal isotropic-nematic phase transition has been studied by means of Monte Carlo simulation. We present equations of state for the isotropic-nematic branches and, in the isotropic phase, numerically calculated values for the virial coefficients B_2, B_3, and B_4. We have studied two models: 11 hard sphere monomers fused in a linear configuration with a reduced bond length of 0.6 and a 15-monomer version of this model in which monomers at one end of the chain become flexible. We have observed spontaneous nematic liquid crystal formation for both of the fully rigid models, and also for models with up to six flexible monomers in the tail. We conclude that molecular flexibility has a strongly destabilizing effect on the nematic phase. This is probably due to the decrease in shape anisotropy that flexible tails allow.

DOI: 10.1103/PhysRevE.64.011703 PACS number(s): 64.70.Md, 83.80.Xz, 61.25.Em, 24.10.Lx

I. INTRODUCTION

It was Onsager [1] in 1949, who demonstrated that one could predict an isotropic-nematic transition in a system whose molecules are modeled by long ''hard'' rods, or in other words, a model that consists only of excluded volume interactions. He showed that for infinitely long rods the isotropic nematic transition occurred at vanishingly small densities. Later, with the advent of the Monte Carlo simulation [2], the molecular dynamics simulation, and the development of fast computing machines, it became possible to study a much greater range of models. In 1985 Frenkel and Mulder [3] demonstrated the formation of a stable nematic phase for a system of hard ellipsoids of revolution using Monte Carlo simulations. Later, in 1988, Frenkel [4] showed the formation of a stable smectic phase for the spherocylinder system, thus revealing the enormous potential of computer simulation in the study of the rich phase behavior of complex fluids. The last 15 years have played host to a wide range of studies, both theoretical and by means of computer simulation, for a great variety of models. For example, hard models that have been investigated include spherocylinders [5–7], hard ellipsoids [3,8], linear chains of tangentially bonded hard spheres (LTHS) [9,10], and the fused hard sphere chain model (FHSC) [11–13]. Liquid crystal formation in systems composed of geometric hard bodies is well documented and we refer the reader to the following reviews [14–16]

Molecules that form liquid crystal phases (especially thermotropic nematic phases) rarely consist solely of a rigid core; they are usually flanked by flexible units either at one or both ends of the core [17]. The study of liquid crystal formation in models that contain flexible units may be considered as a logical progression in the route from the investigation of the mesophasic behavior of hard geometric bodies to the point where one can accurately compute structural and thermodynamic properties for any given mesogenic compound.

There are several ways in which flexibility can be introduced into a model. Flexibility may be introduced homogeneously; typically a model will consist of a number of geometric elements whose relative locations can vary according to some function. Models of this type have been studied by Wilson [18–20], Dijkstra and Frenkel [21], Yethiraj and Fynewever [22], and Fynewever and Yethiraj [23], among others. One of the conclusions drawn from work on such models is that the introduction of flexibility destabilizes the nematic phase with respect to an equivalent fully rigid model. In the case of a completely flexible model, such as that of the ''pearl necklace'' model [24–26] (i.e., a fully flexible tangent hard sphere model), no liquid crystal phase formation is observed. The introduction of flexibility in this manner provides a good starting point for studies of polymeric liquid crystals, which are composed of long chains that have an overall degree of flexibility [27].

Smaller mesogenic molecules are frequently found to be composed of a rigid core (for example, a linear series of benzene rings) which has flexible groups (for example, alkyl chains) attached at either one or both ends of the core section. In this case one can make a clear distinction between a rigid section and a flexible section or sections. In this paper we wish to examine the effect that the addition and the introduction of a flexible tail has on the isotropic-nematic phase transition. With this goal in mind there are a number of possible routes to address this problem. One possibility is to use a realistic model. Examples of studies of this nature can be found in the literature [28–32]. However, the addition of soft potentials, bond bending, bond stretching, and possibly torsional potentials, increases the complexity of the model dramatically. This increase in complexity is reflected in the considerable computational resources required in the study of such models. In this paper we have chosen to study a much simpler model which, although more ''ideal,'' does allow us to study more Hamiltonians than the simulation of a realistic model would permit. This approach has already been taken by other authors [33–35]. The work of Duijneveldt and Allen is particularly interesting [33]. These au-

*Present address: Institut fur Physik, Johannes Gutenberg–Universitat Mainz, WA31, D-55099, Mainz, Germany.

thors have used a hard spherocylinder as the rigid core and an ''ideal'' tail (made up by points which have zero volume and which can not overlap with the spherocylinder) as the flexible unit. They have considered the role of adding the flexible tail and concluded that the smectic phase is stabilized by the addition of the flexible tail. One limitation of their model is the ideal character of the tail since it has zero volume, thus there are no tail-to-tail interactions. It is not clear whether their conclusions hold equally well when the tails become nonideal.

In the early 1980s Wertheim proposed a theory for associating fluids. When the association between sites becomes infinitely strong, chainlike fluids are formed. Starting with the equation of state (EOS) and structural properties of the reference system formed by hard spheres, one can determine the EOS of tangent hard sphere chains by using a perturbative approach. This is usually called first-order thermodynamic perturbation theory or ''TPT1'' theory. This theory was proposed simultaneously by Wertheim [36] and by Chapmann *et al.* [37]. The TPT1 EOS has been extended [38] to the case where a certain degree of overlap is allowed between contiguous monomers of the chain (i.e., when the reduced bond length is less than 1). TPT1 provides us with a good EOS for chains formed from hard spheres. A good EOS for hard sphere chains is important as studies of the isotropic-nematic transition [10,9] rely on the isotropic EOS. However, it must be mentioned that according to Wertheim's TPT1 the EOS of the chains does not depend on chemical details such as bond angle or the presence or absence of flexibility. This surprising result has been tested by comparison with simulation results for short chains, and it has indeed been found that the EOS for short tangent hard sphere chains is hardly affected by molecular flexibility [39].

However, one may suspect that this finding cannot hold true for long chains; fully flexible chains do not form liquid crystal phases whereas fully rigid chains form mesophases. Therefore, for long chains differences between rigid and flexible models must indeed appear.

In this paper we shall study the liquid crystal formation of molecules formed by chains of hard spheres by means of computer simulation. The choice of the model is motivated by the great impact that Wertheim's work has had on literature concerning flexible molecules. We wish to address two issues concerning flexibility. The first issue is the addition of a flexible tail. We do this by comparing a model that consists of a fully rigid linear chain of 11 monomers with a similar model that has a flexible tail of four monomer units. Notice that our tail is nonideal, a difference with respect to the work of Duijneveldt and Allen [33]. The monomers of the flexible tail interact with each other through a hard sphere potential. Second, we shall study the effect of introducing flexibility. For that purpose we shall start with a fully rigid linear chain of 15 monomers and then study the effect that making monomers at one end of the chain fully flexible has on the phase diagram. Therefore when discussing the role of flexibility on phase diagrams we shall make a distinction between ''adding'' flexible tails, or ''introducing'' flexible tails. The model considered in this work has the appealing feature that the rigid and flexible parts of the molecule are formed by the same type of hard sphere monomers, thus the model has an inherent symmetry between the rigid and the flexible part. Another attractive feature is that the model is susceptible to a theoretical treatment based on an extension of Wertheim's work to nematic phases and to molecules that combine rigid and flexible monomer units.

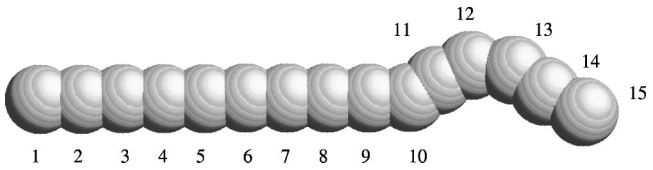

FIG. 1. Model used in this work. Snapshot of a 10+5 RFFFHS molecule in the gas phase.

The format of this paper is as follows: in Sec. II we describe the model in more detail as well as details of the Monte Carlo (MC) simulations. In Sec. III we present the main results of this work for the isotropic phase. In Sec. IV the main results of this work for the isotropic-nematic transition will be presented. Finally our conclusions are presented in Sec. V.

II. MODEL AND COMPUTATIONAL TECHNIQUE

The molecular model used in this work consists of m_r rigid hard spheres (or monomers) followed by m_f flexible hard spheres (or monomers). Each of the monomers are of diameter σ. The total number of hard spheres that constitute the molecule is denoted as m and is given by $m=m_r+m_f$. The relative configuration of the rigid section remains unaltered during the simulation runs. The m_f flexible monomers are subject to Monte Carlo configurational bias. The bond length between monomers is set at $L=0.6\sigma$ thus giving a reduced bond length $L^*=L/\sigma$ of 0.6. The interaction between monomers in different molecules or between nonbonded monomers of the same molecule is of the hard sphere type [40]. There are no bond bending or torsional potentials between the monomers that form the flexible tail. The monomers in the tail may adopt any configuration so long as they are free of intramolecular or intermolecular overlap. In practice the constraint in the bond length to $L^*=0.6$ makes deviations greater than 67.2° impossible for a certain monomer with respect to the vector formed by the two previous monomers of the chain. Overlap checks are made between all nonbonded pairs of atoms, both intermolecular and intramolecular, using the minimum image convention. By doing this, even for intramolecular interactions, we avoid the possibility of overlap between a given molecule and its own image. Since all the interactions in the model are ''hard'' interactions the temperature becomes a redundant variable and the properties of the system depend only on the density. The models used in this work will be denoted as rigid fully flexible fused hard sphere models (RFFFHS). The model is described in more detail in Fig. 1 for the case $m_r=10$, $m_f=5$ (or more succinctly we shall adopt the notation 10+5).

We shall now describe the models studied in this work. First, two fully rigid models have been considered. The length to breadth ratios are 9.4 for the 15+0 model and 7.0

for the 11+0 model. Whittle and Masters [12] found nematic phases for m_r models consisting of eight monomers with $L^*=0.5$ and $L^*=0.6$. Thus we felt certain that the choice of molecules containing 11 and 15 monomer units would provide us with a nematic phases which we could study. The choice of the dimensions for the $m_r+m_f=15$ model were made in a loose relation to the dimensions of the well known mesogen 4-cyano-4′-8-alkyl-biphenyl (8CB).

A fused model has been chosen for two main reasons. First, fusing the spheres increases the convexity of the model with respect to the tangent hard sphere model. Williamson and Jackson [9] have highlighted the possibility of molecules that have a high degree of nonconvexity ''locking'' together in the high density fluid, forming long-lived metastable glassy states. We hope that this effect is reduced due to the more convex nature of our model. Second, the fused model allows for a more gradual introduction of flexibility than would be the case with a tangent hard sphere model.

To analyze the effect of the addition of a flexible tail to a rigid model we then studied the 11+4 model. By comparison of the 11+0 model with the 11+4 we are able to study the effect of adding a flexible tail to a rigid core.

Next we have considered the introduction of flexibility. Starting from the 15+0 model we have introduced a flexible tail while maintaining the total number of monomers of the chain constant at $m=15$. We have studied the 13+2, 11+4, 10+5, 9+6 and 8+7 models. We then compare the results for these models with the 15+0 case. This allows us to see the effect that increasing the region of flexibility within the molecule has while keeping the number of monomers constant.

We have performed the simulations using configurational bias Monte Carlo in the NpT ensemble. The shape of the simulation box was either cubic or orthorhombic. The number of molecules used in all the cases was $N=108$ although for the 15+0 model simulations were also performed for $N=500$ to test for system size dependence. Isotropic scaling of the box dimensins was used throughout the simulation runs except for the 15+0 500 molecule system where anisotropic box scaling was used. Compression of the 108 molecule system is easier than compression of the 500 molecule system due to the higher probability of generating a configuration for which a trial volume move would be acceptable. The types of moves performed on the molecules include translations and rotations. The internal degrees of freedom of the flexible tails were sampled by using the configurational bias algorithm [41]. A cycle includes a trial move per particle (translation 40%, rotation 40%, and configurational bias of the flexible tail 20%) plus a trial change of volume. A typical run comprised of approximately 2×10^5 cycles for equilibration followed by 3×10^5–5×10^5 cycles for production averages. The longer runs were performed for state points that were seen to be near a phase transition.

Our study of the 15+0 model with systems of both 108 and 500 molecules revealed no significant finite size effects. We believe that the main conclusions of this work concerning isotropic-nematic transitions would not be affected by using a larger system.

One drawback of studying systems of just $N=108$ molecules concerns the formation of smectic phases. To study smectic phases much larger systems are required, thus allowing the formation of several smectic layers. For smectic and solid phases nonisotropic NpT simulations should be used. Moreover, when studying smectic and solid phases by means of computer simulation it is a good idea to have the initial configurations defect free [33]. On compressing nematic phases it is possible to observe the spontaneous formation of smectic phases; however, the smectic phases obtained by compression quite often contain defects (for example, molecules often become trapped between layers, lying perpendicular to the layer normal). In our simulations we observe the formation of smectic phases by compression. We shall indicate that when reporting the simulation results. Whereas the spontaneous formation of smectic phases from the nematic phase is an interesting feature we recommend caution when analyzing the actual values of the densities at which this transition appears. Those densities will certainly be affected when larger systems are considered, and when defect-free smectic configurations are used.

We would like to stress at this point that the main goal of this work is to study the role of flexible tails on the isotropic-nematic transition and our results concerning the nematic-smectic transition are just preliminary for the reasons described above.

During the simulations the nematic order parameter (which is zero for an isotropic fluid and one for a perfectly aligned system) was continuously monitored. This was done by first calculating a director vector [42]

$$Q_{\alpha\beta}=\frac{1}{N}\sum_{j=1}^{N}\left(\frac{3}{2}\hat{e}_{j\alpha}\hat{e}_{j\beta}-\frac{1}{2}\delta_{\alpha\beta}\right),\quad \alpha,\beta=x,y,z, \tag{1}$$

where Q is a second rank tensor, $\hat{\mathbf{e}}_j$ is a unit vector along the long axis (defined as the eigenvector associated with the largest eigenvalue of the inertia tensor) of the molecule, and $\delta_{\alpha\beta}$ is the Kronecker delta. Diagonalization of this tensor gives three eigenvalues λ_+, λ_0, and λ_-, and $\mathbf{n}$ is the eigenvector associated with the largest eigenvalue (λ_+). From this director vector the nematic order parameter is calculated from [43]

$$S_2=\lambda_+=\langle P_2(\mathbf{n}\cdot\mathbf{e})\rangle=\langle P_2(\cos\theta)\rangle=\left\langle\frac{3}{2}\cos^2\theta-\frac{1}{2}\right\rangle, \tag{2}$$

where S_2 is known as the uniaxial order parameter. Here P_2 is the second-order Legendre polynomial, θ is the angle between a molecular axes and the director $\mathbf{n}$, and the angular brackets indicate an ensemble average. As well, the nematic order parameter snapshots of simulation configurations were also taken for use as an aid to phase identification.

The simulations were performed as follows: for each model we started from a very low density state. The initial configuration was that of the α face-centered-cubic structure [40], thus the initial nematic order parameter was zero and no preferential direction to the molecules was artificially introduced. Within a few steps the solid melts and is transformed into a low density isotropic fluid. We then proceed to

TABLE I. Calculated virial coefficients for the isotropic phase.

m_r	m_f	B_2^*	B_3^*	B_4^*	$B_3^*/(B_2^*)^2$	$B_4^*/(B_2^*)^3$
15	0	12.906±0.002	55.859±0.03	−9.058±0.26	0.335	−0.0042
14	1	12.854±0.003	56.161±0.03	−2.842±0.214	0.340	−0.0013
13	2	12.737±0.008	56.504±0.02	5.461±0.14	0.348	0.0026
12	3	12.602±0.006	56.805±0.08	14.594±0.31	0.358	0.0073
11	4	12.469±0.015	57.208±0.03	23.285±0.86	0.368	0.0120
10	5	12.239±0.008	57.512±0.14	36.567±0.60	0.384	0.0199
9	6	12.115±0.019	57.946±0.12	46.061±0.91	0.395	0.0259
8	7	11.879±0.003	58.201±0.13	60.548±1.02	0.412	0.0361

compress this fluid by increasing the pressure. The last configuration from a certain pressure was used as an initial configuration for the next, higher, pressure. States for which the nematic order parameter was greater than 0.4 were classified as being nematic. All states obtained from compression of a low density isotropic fluid will be denoted as compression states.

In addition to compression states, expansion runs were also performed. Let us briefly describe how the expansion runs were undertaken. The system most likely to spontaneously form a nematic phase from the isotropic fluid was the 15+0 model. Once a high density nematic phase was obtained for the 15+0 model this configuration was used as the initial configuration for the nematic phase for a model that incorporated flexibility (i.e., the 13+2 model). The only precaution is to locate half of the flexible tails up, and half of the flexible tails down with respect to the nematic director directions. This is important if one wishes to avoid the possibility of forming an artificial ferroelectric nematic (with all the tails up or down). We did not observe, in any compression runs, the formation of ferroelectric nematic phases and therefore this phase does not appear in the phase diagram of the models considered in this work.

Once the nematic phase for the 13+2 model had been equilibrated we then proceeded to expand the system by decreasing the pressure. We shall denote these runs as expansion runs. The high density nematic configuration obtained for the 13+2 model was used as an initial configuration of the nematic phase of the 11+4 model. From this configuration we proceeded to expand the nematic phase of the 11+4 model. Therefore our runs can be divided into compression runs, which were obtained from a low density gas isotropic phase, and expansion runs which were obtained by expanding a high density nematic configuration.

In addition to the NpT Monte Carlo simulations described so far we have also evaluated the virial coefficients of those models in the isotropic phase. In the isotropic phase the second, third, and fourth virial coefficients were calculated for each of the models from 15+0 to 8+7 inclusive. This was done by following the method proposed by Vega [44]. For a complete description of the means of calculating the virial coefficients the reader is referred to the aforementioned paper. In summary one treats the fluid as a multicomponent mixture, where each conformation represents a distinct mixture component. We performed a Monte Carlo simulation on an individual molecule. The simulation consisted of 4×10^7 Monte Carlo passes. Every 1×10^4 passes the instantaneous configuration was written to a file thus obtaining 4000 configurations. From this set of 4000 configurations four different conformations were selected randomly and the virial coefficients were calculated for those selected conformers. This is repeated 1600 times and the average value of the virial coefficients is calculated.

III. RESULTS FOR THE ISOTROPIC PHASE

In this section results will be reported for the isotropic phase. We shall divide the results into two sections; the first section corresponds to the low density region and the second section to the medium density region.

A. The low density region

The equation of state of a fluid can be described in terms of the compressibility factor Z, where $Z=p/(\rho kT)$, with p being the pressure, $\rho=N/V$ the number density of the fluid (number of molecules per unit of volume), k is the Boltzmann constant, and T is the temperature. The compressibility factor can be expanded in powers of the packing fraction $y=\rho V_m$, where V_m is the molecular volume. The volume of a linear chain of m hard spheres of diameter σ and of bond length L is given by [45]

$$V_m=\frac{\pi}{6}\sigma^3\left\{1+\frac{(m-1)}{2}\left[\frac{3L}{\sigma}-\left(\frac{L}{\sigma}\right)^3\right]\right\}. \tag{3}$$

The coefficients of the expansion of Z in powers of y receive the name of virial coefficients and will be denoted as B_n. As the model is a hard body the compressibility factor is temperature independent, hence the EOS is given by

$$Z=1+B_2^*y+B_3^*y^2+B_4^*y^3+\cdots, \tag{4}$$

where

$$B_n^*=B_n/V_m^{n-1}. \tag{5}$$

For hard convex bodies the second virial coefficient can be calculated exactly [46]. However, the model used in this study is nonconvex, thus we have to numerically calculate B_2,B_3, and B_4 by using the procedure described in the preceding section.

In Table I the second, third, and fourth virial coefficients

of the RFFFHS models (with $m=15$) considered in this work are reported. Each of the models has the same molecular volume. As can be seen the introduction of flexibility in the model significantly modifies the virial coefficients. Let us now analyze in detail each of the virial coefficients. The second virial coefficient decreases slightly as the molecular flexibility increases. Since the second virial coefficient is a measure of the volume excluded to a second molecule by the presence of the first molecule, it can be concluded that rigid linear molecules present a greater excluded volume than flexible ones. For hard convex bodies the second virial coefficient is given exactly by the equation [46]

$$B_2^* = 1 + 3\alpha, \tag{6}$$

where α is the parameter of nonsphericity which can be evaluated from geometrical considerations. For hard spheres $\alpha=1$; for all other hard convex bodies $\alpha>1$. In other words, the more ''nonspherical'' a body is, the larger its value of α and hence of B_2^* is. The molecules considered in this work are nonconvex, thus Eq. (6) no longer holds; however, it can be used to explain, in a general fashion, the results of Table I for B_2^*. These results indicate that in the isotropic phase the molecules become more spherical as the flexibility of the molecule increases.

Concerning B_3^* one can observe that the introduction of flexibility slightly changes its value (we see an increase of about 4% with flexibility) though the third virial coefficient seems to be less sensitive to the introduction of flexibility than the second and the fourth virial coefficients. That has also been noted by Vega *et al.* [47] for tangent hard sphere models.

We find a dramatic change in B_4^* with the introduction of flexibility. From Table I we see that B_4^* changes from negative to positive values as the molecule becomes more flexible. Negative values of the fourth virial coefficient are common for highly prolate molecules [48,49]. Therefore the negative values found for the $15+0$ and $14+1$ models are not surprising. Previously this has been attributed to the dominance of the ''modified star graph'' in the Ree and Hoover formulation [48].

In summary the results of Table I show that the virial coefficients are affected by the Introduction of flexibility in the molecular model. The third and especially the fourth virial coefficients increase as the molecule becomes more flexible, while the second virial coefficient decreases.

It was mentioned in the Introduction of this paper that Wertheim [36] and Chapmann *et al.* [37] have proposed an EOS for chains of tangent hard sphere fluids. The EOS obtained in this way, denoted usually as TPT1, predicts that the EOS and hence the virial coefficients are independent of the presence or absence of molecular flexibility. This equation reads

$$Z = \frac{p}{\rho kT} = m\frac{1+y+y^2-y^3}{(1-y)^3} - (m-1)\frac{1+y-\frac{y^2}{2}}{(1-y)\left(1-\frac{y}{2}\right)}, \tag{7}$$

where m is the number of tangent hard spheres forming the chain. From this equation one can obtain expressions for the second, third, and fourth virial coefficients [50]

$$B_2^{*,\mathrm{TPT1}} = 1.5m + 2.5, \tag{8}$$

$$B_3^{*,\mathrm{TPT1}} = 7.25m + 2.75, \tag{9}$$

$$B_4^{*,\mathrm{TPT1}} = 15.125m + 2.875. \tag{10}$$

Although Eq. (7) is designed for a tangent hard sphere chain, Zhou and co-workers [38] have developed an expression for an effective number of monomer units, m_{eff}, which allows TPT1 to be applied to models of fused hard sphere chains, for $L^* \geqslant 0.5$. This is given by

$$m_{\mathrm{eff}} = \frac{[1+(m-1)L^*]^3}{[1+(m-1)L^*(3-L^{*2})/2]^2}. \tag{11}$$

From Eq. (11) for the model described in this paper (RFFFHS with $m=15$) $m_{eff} \approx 5.6843$, which gives

$$B_2^{*,\mathrm{TPT1}} \approx 11.02, \tag{12}$$

$$B_3^{*,\mathrm{TPT1}} \approx 43.96, \tag{13}$$

$$B_4^{*,\mathrm{TPT1}} \approx 88.85. \tag{14}$$

From a comparison with the results from this study (Table I) we see that TPT1 underestimates B_2^* and B_3^* and overestimates B_4^*. The lack of reference to molecular flexibility within TPT1 means that these values are invariant with respect to the changes in the flexibility that we introduce in our model. To summarize TPT1 is not able to capture the subtle changes occurring in the virial coefficient when molecular flexibility is introduced into the model.

Let us now present results for Z at low densities. In Fig. 2 the compressibility factor Z is shown as a function of y for volume fractions up to 0.2. The results presented were obtained from the virial expansion truncated at B_4, from TPT1, and from computer simulations of this work. Results correspond to two models, namely $15+0$ and $11+4$. As can be seen the virial expansion reproduces the simulation results rather well, whereas TPT1 fails in describing the low density region. The virial expansion correctly reproduces the slightly smaller value of Z for the $15+0$ model with respect to the $11+4$ model. One can summarize by saying that although virial coefficients are significantly affected by the introduction of flexibility the increases in the third and fourth virial coefficients are offset by the decrease in the second virial coefficient, hence we see little change in the virial expansion between each of the models. At higher packing fractions ($y>0.20$), the truncated virial expansion significantly underestimates the compressibility factor. The inclusion of higher virial coefficients would be required in order to provide a better description of the higher density region.

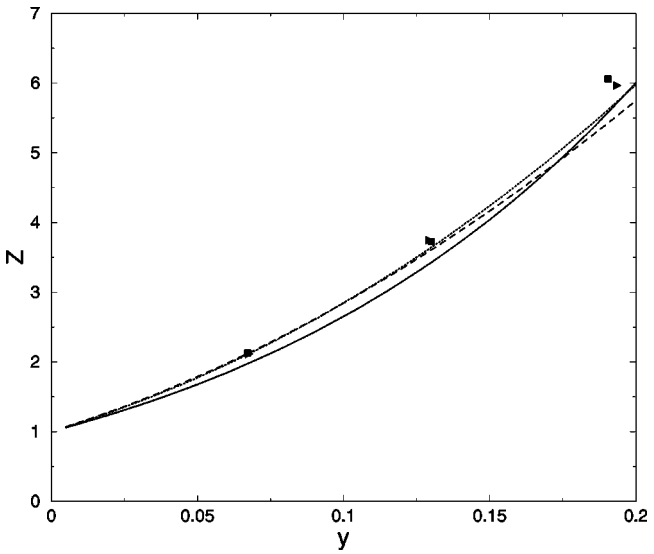

FIG. 2. Monte Carlo results (compressibility factor versus volume fraction) of the RFFFHS models (symbols) in the low density region of the isotropic phase; ■, 11+4 (isotropic); ▶, 15+0 (isotropic). The equation of state obtained from the virial expansion is also presented, 11+4 virial expansion (dotted line), 15+0 virial expansion (dashed line). The solid line represents the TPT1 EOS using the Zhou *et al.* [38] ''correction''.

B. The medium density region

We shall now present results for the isotropic phase at medium densities (namely those with $y>0.20$). In Fig. 3 the EOS in the isotropic region as obtained from TPT1 and from the simulation results of this work are plotted. As can be seen TPT1 performs very well in this region. In fact at medium densities (in the isotropic phase) TPT1 correctly predicts that the EOS is hardly affected by the introduction of molecular flexibility.

The success of TPT1 in the isotropic phase at medium densities strongly suggests that this theory could be used for theoretical treatments concerning the isotropic-nematic transition. This has been illustrated by Williamson and Jackson [9] for fully rigid tangent hard spheres. We feel that this theory could be extended to the RFFFHS model by numerical or analytical [11] calculation of the excluded volume.

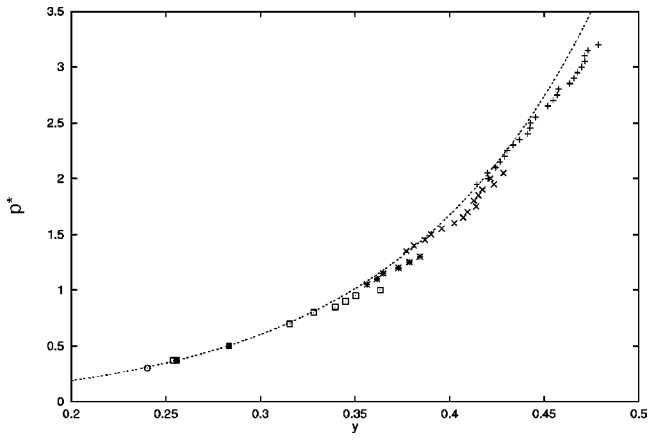

FIG. 3. Monte Carlo results [reduced pressure $p^*=p\sigma^3/(kT)$ versus volume fraction] for the EOS of the RFFFHS models in the isotropic phase at medium densities (symbols). Results correspond to +, 8+7; ×, 9+6; *, 10+5; □, 11+4; ■, 13+2; and ○, 15+0. The dashed line represents the TPT1 EOS using the Zhou *et al.* ''correction''.

TABLE II. Equation of state for the 11+0 model from NpT MC simulations. The reduced pressure p^* is defined as $p^*=p\sigma^3/(kT)$, Z stands for the compressibility factor, y for the volume fraction, S_2 for the order parameter. The different phases have been labeled as I (isotropic), N (nematic), and Sm (smectic).

p^*	y	Z	S_2	Phase
0.10	0.138	3.37	0.10	I
0.20	0.191	4.89	0.09	I
0.40	0.255	7.34	0.08	I
0.50	0.277	8.43	0.19	I
0.60	0.296	9.45	0.12	I
0.65	0.306	9.92	0.15	I
0.70	0.319	10.26	0.09	I
0.75	0.333	10.52	0.58	N
0.80	0.346	10.80	0.66	N
0.85	0.354	11.22	0.77	N
0.90	0.368	11.43	0.73	N
0.95	0.376	11.80	0.81	N
1.00	0.386	12.09	0.87	N
1.05	0.393	12.47	0.85	N
1.10	0.400	12.86	0.90	N
1.15	0.426	12.60	0.96	N

IV. THE ISOTROPIC-NEMATIC TRANSITION

In this section we shall focus on the results for the isotropic-nematic transition. This section will be divided into three sections. In Sec. IV A results for fully rigid models will be presented, namely the 15+0 and the 11+0. In Sec. IV B we shall analyze the effect of adding a flexible tail. To do this we shall compare the results for the 11+0 model with the 11+4 model. Finally, in Sec. IV C we shall analyze the effect of introducing flexibility and present the results for the 15+0, 13+2, 10+5, 9+6, and 8+7 models.

A. Isotropic-nematic transition of fully rigid models

First we shall present the results for the 11+0 and 15+0 models. Results for the 11+0 model are given in Table II and the results for the 15+0 model are given in Table III for $N=108$ and in Table IV for $N=500$. In all the cases reported results correspond to compression runs.

On compression of the isotropic phase a nematic phase spontaneously forms at a packing fraction of $y\approx0.33$ for the 11+0 model (Table II). For the 15+0 model the phase transition occurred at a packing fraction of $y\approx0.28$. Whittle and Masters found a nematic phase for the 8+0 model at $y=0.42$. Obviously as the molecule becomes more elongated the isotropic-nematic transition occurs at lower volume fractions. This is also found for hard ellipsoids, hard spherocylinders, and other hard bodies.

TABLE III. Equation of state for the 15+0 model from NpT MC simulations (108 molecules). The notation is as in Table II.

p^*	y	Z	S_2	Phase
0.02256	0.067	2.10		I
0.07652	0.129	3.74		I
0.18233	0.193	5.95		I
0.30	0.240	7.90	0.13	I
0.35	0.276	8.01	0.78	N
0.40	0.296	8.52	0.81	N
0.45	0.314	9.04	0.88	N
0.50	0.332	9.52	0.90	N
0.55	0.345	10.07	0.89	N
0.60	0.359	10.56	0.92	N
0.65	0.379	10.83	0.95	N
0.70	0.382	11.58	0.95	N

TABLE IV. Equation of state for the fully rigid 15+0 model from NpT MC simulations (500 molecules). The notation is as in Table II.

p^*	y	Z	S_2	Phase
0.10	0.147	4.31	0.05	I
0.25	0.219	7.24	0.08	I
0.35	0.255	8.68	0.08	I
0.45	0.297	9.60	0.75	N
0.50	0.332	9.54	0.84	N
0.55	0.346	10.06	0.87	N
0.60	0.359	10.58	0.89	N
0.65	0.370	11.13	0.90	N
0.70	0.376	11.78	0.92	N
0.75	0.392	12.09	0.93	N
0.80	0.401	12.61	0.94	N
0.85	0.418	12.86	0.95	N
0.90	0.425	13.40	0.96	N
0.95	0.441	13.62	0.97	Sm-A
1.00	0.465	13.61	0.96	Sm-A

It is interesting to compare the densities at which the nematic phase forms for the RFFFHS model considered in this work with the densities at which the nematic phase forms for other hard bodies, such as spherocylinders [7] or linear tangent hard spheres [9]. A comparison is made in Table V for models having the same length-to-breadth ratio. Let us start by comparing spherocylinders with the model of this work. Spherocylinders are found to form a nematic phase at higher volume fractions than the model used in this study. This is true for the two length-to-breadth ratios presented in Table V. This is a consequence of the fact that B_2^* of spherocylinders is lower than B_2^* of the RFFFHS model having the same length-to-breadth ratio. The nonconvex character of the model of this work means that a sphere sliding on the surface of the molecule cannot efficiently penetrate the cavities between two monomer sites [45]. This is not the case for the spherocylinder where a sphere can slide easily over the surface of the spherocylinder. This is reflected in the values of B_2^*. Also in Table V the results for linear tangent hard spheres are presented. As can be seen the results of this work are in fair agreement with those reported by Williamson and Jackson. We conclude that the phase behavior of models presented in this work lies between that of the linear tangent hard sphere model and the spherocylinder model. Notice that by keeping the length-to-breadth ratio constant and increasing the number of spheres of the model (and correspondingly reducing the bond length) the model of this work should tend to the spherocylinder limit. The way in which the spherocylinder limit is obtained from models of hard spheres has been considered in more detail by Jaffer, Opps, and Sullivan [11].

In this work we have not made a systematic study of the influence of system size dependence on the results. The only model for which larger systems were considered was the 15+0 model. The results of this model for $N=108$ and $N=500$ are shown in Fig. 4. We do not observe any significant differences in the EOS in the isotropic phase.

In both systems a nematic phase is formed spontaneously although it appears at slighter higher densities for the system with $N=500$. This shift of the phase transition to a slightly higher density is expected since the phase transition occurs when orientational correlations are commensurate with the dimensions of the simulation box, which are slighty larger for the 500 molecule system. In the nematic phase we do not observe any significant differences in the EOS between the two systems. For densities higher than $y>0.41$ we observe that the system with $N=108$ is attempting to form a smectic phase (identified by analyzing the snapshots of the system and by a kink in the EOS), but the size of the system prevents the formation of a conclusive smectic phase. When compressing the system with $N=500$ a smectic-A phase

TABLE V. Packing fractions at which the isotropic-nematic transition occurs for spherocylinders, the model of this work, and the rigid tangent linear hard sphere model. The length-to-breadth ratio of the model is denoted as γ.

Model	Study	γ	I-N transition
Spherocylinder	Bolhuis and Frenkel [7]	9.4	$0.29 \leqslant y \leqslant 0.32$
Our model 15+0		9.4	$0.26 \leqslant y \leqslant 0.29$
Spherocylinder	Bolhuis and Frenkel [7]	7.0	$0.36 \leqslant y \leqslant 0.37$
Our model 11+0		7.0	$0.32 \leqslant y \leqslant 0.33$
THS	Wiliamson and Jackson [9]	7.0	$0.303 \leqslant y \leqslant 0.312$ (on compression)
THS	Wiliamson and Jackson [9]	7.0	$0.285 \leqslant y \leqslant 0.304$ (on expansion)

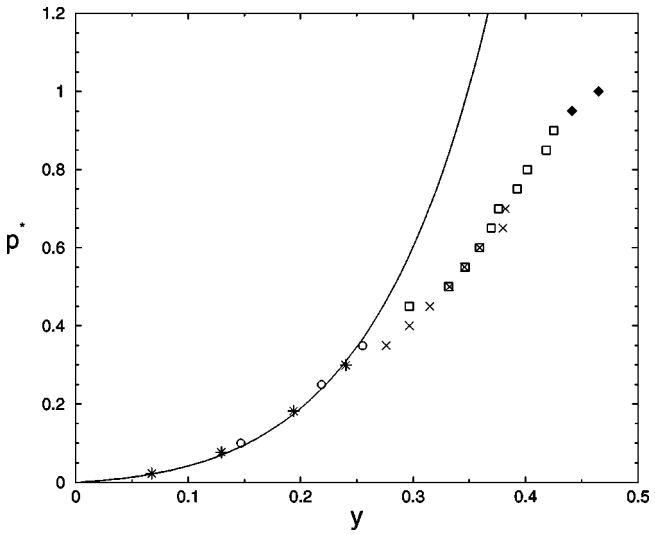

FIG. 4. The equation of state from the MC simulations. ○, 15+0 500 molecules (isotropic); □, 15+0 500 molecules (nematic); ◆, 15+0 500 molecules (smectic); *, 15+0 108 molecules (isotropic); ×, 15+0 108 molecules (nematic). The curve represents the TPT1 EOS using the Zhou *et al.* correction.

spontaneously forms at $y>0.43$. This is more clearly illustrated by showing a snapshot of the system (Fig. 5).

In summary the influence of system size in the EOS of the isotropic and nematic phases is quite small and the same is true for the isotropic-nematic transition. However, system size effects are important when considering the nematic-smectic transition. Although the system with $N=108$ gives some indications of a transition to a smectic phase only the larger system with $N=500$ formed a truly smectic phase. We shall describe our results for smectic phases as being preliminary.

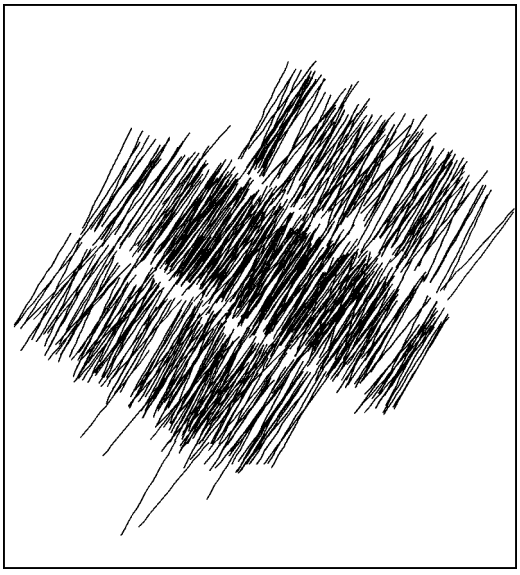

FIG. 5. A snapshot of the 15+0 model in the smectic-*A* phase for a system of 500 molecules.

TABLE VI. Equation of state for the 11+4 model from *NpT* MC simulations (compression runs). The notation is as in Table II. The square root of the average squared end-to-end distance is denoted as $\langle R^2\rangle^{1/2}$ and is given in σ units. The notation *N*/Sm indicates that the transition from the nematic to the smectic phase is taking place.

p^*	y	Z	S_2	$\langle R^2\rangle^{1/2}$	Phase
0.02260	0.067	2.12		7.2052	*I*
0.07652	0.130	3.72		7.1969	*I*
0.18233	0.190	6.05		7.1914	*I*
0.37136	0.253	9.25		7.1949	*I*
0.70	0.315	14.04	0.15	7.2269	*I*
0.80	0.328	15.43	0.11	7.2217	*I*
0.85	0.339	15.84	0.05	7.2237	*I*
0.90	0.345	16.51	0.13	7.2391	*I*
0.95	0.350	17.16	0.25	7.2407	*I*
1.00	0.363	17.42	0.35	7.2941	*I*
1.05	0.373	17.80	0.76	7.3557	*N*
1.10	0.380	18.28	0.68	7.3746	*N*
1.15	0.384	18.94	0.79	7.3531	*N*
1.20	0.390	19.47	0.74	7.3641	*N*
1.25	0.396	19.95	0.70	7.3660	*N*
1.30	0.408	20.16	0.70	7.4200	*N*/Sm
1.35	0.415	20.56	0.78	7.4298	*N*/Sm
1.40	0.422	20.95	0.76	7.4283	*N*/Sm
1.45	0.434	21.11	0.79	7.4278	*N*/Sm
1.50	0.438	21.64	0.77	7.4494	*N*/Sm
1.55	0.444	22.05	0.80	7.4299	Sm
1.60	0.449	22.50	0.81	7.4596	Sm
1.65	0.453	23.02	0.82	7.4639	Sm

B. Adding a flexible tail

We shall now analyze the effect of adding a flexible tail to the 11+0 model. In particular we shall consider the 11+4 model in which a tail consisting of four monomer units is added to the rigid core of 11 monomers. In principle one would expect that the addition of a flexible tail would hinder liquid crystal phase formation; fully flexible models do not have liquid crystal phases at all. However, due to the bond length constraint $L^*=0.6$ and the condition of no intramolecular overlap the tail is not as flexible as it may first appear. In fact each flexible bond can deviate only 67° from the direction of the previous bond to avoid overlap between site n and site $n-2$. Therefore, linear configurations are still possible and it is not clear whether the main effect of adding the tail is to increase the overall molecular elongation thus making the formation of the liquid crystal phase easier.

The simulations results for the 11+4 model are presented in Table VI. It can be seen that a nematic phase is formed at $y\approx0.37$. Since for the 11+0 model the nematic phase is formed at $y\approx0.33$ one concludes that the addition of a flexible tails moves the isotropic-nematic transition to higher densities. The effect is important. Therefore the addition of a flexible tail makes the nematic phase less stable. In Table VI results for the square root of the mean squared end-to-end distance, $\langle R^2\rangle^{1/2}$, are also shown. Structural changes are ob-

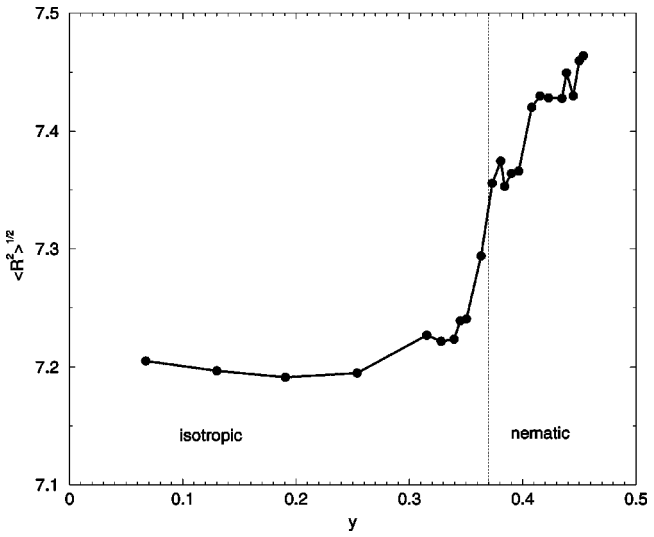

FIG. 6. A plot of the mean end-to-end length (in σ units) against packing fraction for the 11+4 model.

served when going from the isotropic to the nematic phase. In particular an increase is seen in the end-to-end distance when moving to the nematic phase. This is more clearly seen in Fig. 6 where $\langle R^2\rangle^{1/2}$ is shown as a function of the density for the 11+4 model.

The increases in $\langle R^2\rangle^{1/2}$ correspond to a preference for a more linear configuration in the nematic phase. The tails tend to be aligned with the nematic director in the nematic phase. This effect has been noted in previous studies [31].

In Fig. 7 the EOS for the 11+4 and the 11+0 models are compared. The shift of the isotropic-nematic transition to higher densities is clearly seen. For the 11+4 system we observe a stable nematic phase for volume fractions in the range $0.37<y<0.41$. However, for higher densities the system forms a smectic phase. Smectic phases were identified by graphical visualization. A kink is observed in the EOS at

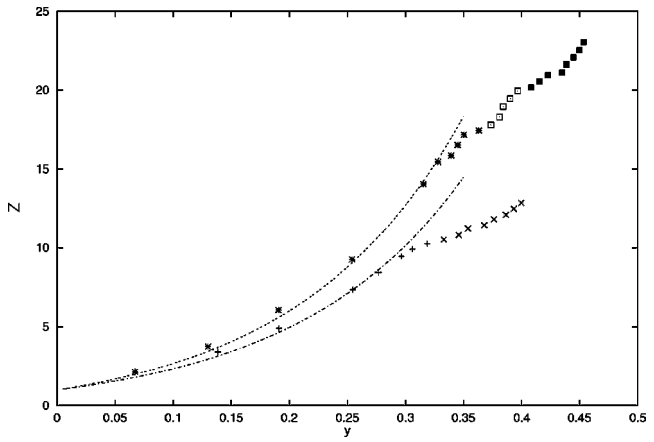

FIG. 7. The equation of state from the MC simulations. *, 11+4 (isotropic); □, 11+4 (nematic); ■, 11+4 (smectic); +, 11+0 (isotropic); ×, 11+0 (nematic). The dotted curve represents the TPT1 EOS for the 15+0 RFFFHS model using the Zhou *et al.* correction. The dot-dashed curve represents the TPT1 EOS for the 11+0 RFFFHS model using the Zhou *et al.* correction.

$y\approx 0.41$. Although our results for smectic phases are preliminary due to the small size of our system ($N=108$), there is strong indication of formation of a smectic phase for the 11+4 system when $y>0.41$. In the observed smectic phases the rigid cores form layers, whereas the flexible tails fill the space between the layers. This is similar to the behavior found by Duijneveldt and Allen for spherocylinders which have ideal tails [33].

We find that the range for which a nematic phase is stable is much smaller in the 11+4 model than in the 11+0 model for two reasons. First because the isotropic-nematic transition has moved to higher densities. Secondly because the nematic-smectic transition seems to be moving to lower densities when the flexible tails are added. To summarize: the addition of flexible tail shifts the isotropic-nematic transition to higher densities, and stabilizes the smectic phase, thus significantly reducing the range of densities where the nematic phase is stable.

C. Introducing flexibility

We shall now analyze the changes that occur when monomers of a fully rigid model become flexible. We shall start from the 15+0 model and will change the last m_f monomers of the model to allow for flexibility.

Let us start with the limiting case. Since fully flexible chains do not form liquid crystal phases one may expect that when m_f is large enough no liquid crystal phase would be observed. In the 8+7 model the length-to-breadth ratio of the rigid core is about 5σ. The anisotropy of the rigid core is still significant. Whittle and Masters observed a nematic phase for the 8+0 model. In Table VII the EOS for the 8+7 as obtained from compression runs is presented. It can be seen that even for volume fractions as high as $y=0.48$ the system remains in the isotropic phase. No nematic phase is formed when compressing this system. For the highest densities the fluid configurations, although isotropic, are of glassy character indicating the vicinity of the fluid-solid transition. The conclusion then is that when a sufficient number of the monomers in the chain are flexible the liquid crystal phase disappears completely from the phase diagram. Obviously one would anticipate the same results for the models with $m_f>7$. What happens when the number of flexible monomers is small and the rigid region of the molecule is big ?

Let us start with the results for the 13+2 model. Results from compression runs from the isotropic fluid are presented in Table VIII. It can be seen that a nematic phase is spontaneously formed at a volume fraction of about $y=0.33$. We also performed expansion runs. The expansion runs were performed as follows. We started from a nematic configuration of the 15+0 model with $y=0.35$. Then we introduced the flexible tails, with half of the molecules having the tail up and half of the molecules having the tail down (with respect to the nematic director). Several long runs are then performed to allow the system to equilibrate at this density. Then, taking this equilibrated configuration as the initial state, several runs were performed by slowly decreasing the pressure. Another set of runs were launched from the initial

TABLE VII. Equation of state for the 8+7 model from NpT MC simulations (compression runs). The notation as in Tables II and VI.

p^*	y	Z	S_2	$\langle R^2\rangle^{1/2}$	Phase
1.95	0.414	29.79	0.27	6.0304	I
2.00	0.420	30.12	0.09	6.0534	I
2.05	0.420	30.90	0.17	6.0111	I
2.10	0.424	31.33	0.21	6.0059	I
2.15	0.427	31.90	0.23	5.9603	I
2.20	0.429	32.45	0.20	5.9585	I
2.25	0.430	33.09	0.10	6.0020	I
2.30	0.434	33.58	0.16	5.9735	I
2.35	0.437	34.03	0.14	5.9721	I
2.40	0.441	34.42	0.13	6.0326	I
2.45	0.442	35.05	0.16	6.0656	I
2.50	0.443	35.73	0.15	6.0146	I
2.55	0.445	36.25	0.17	6.0063	I
2.65	0.452	37.11	0.20	6.1276	I
2.70	0.455	37.58	0.20	5.9808	I
2.75	0.457	38.10	0.23	5.9987	I
2.80	0.458	38.73	0.34	5.9713	I
2.85	0.464	38.91	0.37	6.0630	I
2.90	0.466	39.41	0.24	6.1981	I
2.95	0.467	39.94	0.25	6.1039	I
3.00	0.470	40.42	0.14	6.0256	I
3.05	0.472	40.93	0.21	6.0793	I
3.10	0.471	41.63	0.23	6.1319	I
3.15	0.473	42.15	0.16	6.1019	I
3.20	0.479	42.31	0.14	6.1787	I

configuration by slowly increasing the pressure. Results obtained in this way are presented in Table IX. The line dividing the results in Table IX separates the compression from the expansion runs. By decreasing the pressure we observed a nematic-isotropic transition for $y\approx 0.31$. The existence of hysteresis loops (i.e., the nematic phase is obtained by compression at slightly higher densities than the densities at which the isotropic phase appears by expansion) is usual in first-order phase transitions. Therefore the 13+2 system presents an isotropic-nematic transition at volume fractions of about $y\approx 0.32$. Taking into account that the nematic phase of the 15+0 models appears for volume fractions of about $y\approx 0.28$ we see that the effect of introducing a flexible tail is to shift the transition to higher densities. When compressing the nematic phase a smectic phase appears for volume fractions of about $y=0.42$. Our simulations show that the 13+2 model has a stable nematic phases for volume fractions in the range $0.32<y<0.42$.

TABLE VIII. Equation of state for the 13+2 model from NpT MC simulations (compression runs). The notation is as in Tables II and VI.

p^*	y	Z	S_2	$\langle R^2\rangle^{1/2}$	Phase
0.55	0.297	11.72	0.20	7.9590	I
0.60	0.306	12.42	0.12	7.9572	I
0.65	0.331	12.43	0.83	7.9965	N

TABLE IX. Equation of state for the 13+2 model from NpT MC simulations (expansion and compression runs seeded from a nematic configuration). The notation is as in Tables II and VI. The line dividing the results in the table divides the compression from the expansion runs.

p^*	y	Z	S_2	$\langle R^2\rangle^{1/2}$	Phase
0.02260	0.067	2.11		7.9464	I
0.07652	0.130	3.71		7.9459	I
0.18233	0.192	5.98		7.9460	I
0.37136	0.255	9.19		7.9503	I
0.50	0.283	11.14	0.11	7.9517	I
0.55	0.307	11.32	0.48	7.9775	N
0.60	0.317	11.96	0.62	7.9786	N
0.65	0.336	12.22	0.78	8.0023	N
0.70	0.344	12.85	0.82	8.0054	N
0.80	0.361	14.01	0.82	8.0160	N
0.85	0.374	14.36	0.84	8.0194	N
0.90	0.380	14.95	0.90	8.0253	N
0.95	0.393	15.28	0.90	8.0315	N/Sm
1.00	0.409	15.46	0.95	8.0268	N/Sm
1.05	0.423	15.69	0.96	8.0368	N/Sm
1.10	0.429	16.22	0.96	8.0344	N/Sm
1.15	0.433	16.78	0.94	8.0383	N/Sm
1.20	0.444	17.06	0.96	8.0383	Sm-A

We now move on to the 10+5 system. In Table X results obtained by compression of the isotropic fluid phase are presented. A nematic phase is formed at $y\approx 0.39$ (for the 15+0 model the nematic phase appears for $y\approx 0.28$). Therefore introducing a flexible tail of five monomer units moves the isotropic-nematic transition to much higher densities. This mirrors the trend already observed for the 13+2 model and

TABLE X. Equation of state for the 10+5 model from NpT MC simulations (compression runs). The notation is as in Tables II and VI.

p^*	y	Z	S_2	$\langle R^2\rangle^{1/2}$	Phase
1.05	0.356	18.65	0.20	6.8092	I
1.10	0.361	19.25	0.11	6.7993	I
1.15	0.365	19.95	0.11	6.8036	I
1.20	0.373	20.37	0.15	6.8270	I
1.25	0.379	20.89	0.16	6.8340	I
1.30	0.384	21.41	0.36	6.8514	I
1.35	0.386	22.14	0.41	6.8717	N
1.40	0.395	22.58	0.45	6.9197	N
1.45	0.404	22.45	0.46	6.9460	N
1.50	0.406	23.38	0.55	6.9379	N
1.55	0.415	23.63	0.67	6.9925	N
1.60	0.418	24.23	0.80	7.0466	N/Sm
1.65	0.435	23.98	0.79	7.1019	Sm

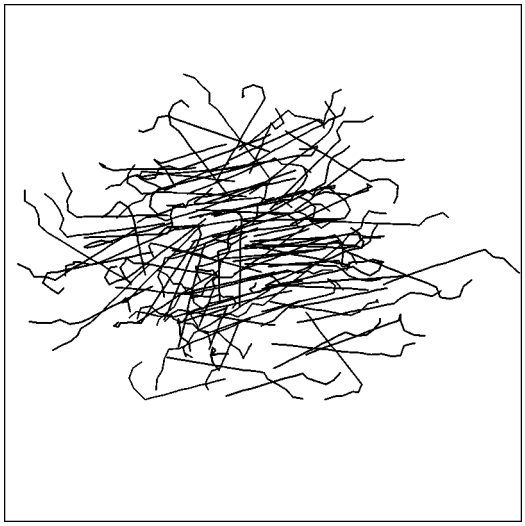

FIG. 8. A snapshot of the 10+5 model in the nematic phase for a system of 108 molecules.

is confirmed by the 10+5 model. A snapshot of the nematic phase formed is given in Fig. 8. This snapshot was obtained from compression of the isotropic fluid.

It can be seen that the tails are up and down with respect to the nematic director direction. When compressing the nematic phase of the 10+5 model some indications of the formation of a smectic phase for $y=0.42$ are observed. In summary, for the 10+5 model the stability range of the nematic phase seems to be quite small, $0.39<y<0.42$.

Let us now focus on the last model considered in this work. This is the 9+6 model. This model is interesting for two reasons. First because it is sandwiched between the 8+7 which, as discussed previously, has no liquid crystal phases, and the 10+5 which does present liquid crystal phases. It is not clear whether the 9+6 model will or will not exhibit liquid crystal behavior. Second, even assuming that the 9+6 model has liquid crystal phases it is not clear whether it will or will not have a stable nematic phase. Taking into account the narrow range of stability of the nematic phase for the 10+5 model the possibility of going directly from the fluid to a smectic phase appears as a possible scenario.

In Table XI the EOS as obtained by compression of the isotropic phase is presented. A nematic phase is formed spontaneously for $y=0.435$. We also perform a second type of run; starting from a smectic configuration of the 10+5 model with $y=0.44$ we switched to the 9+6 model. Several runs were then performed to equilibrate the initial configuration. We then performed a series of expansion and compression runs. Results from these runs are shown in Table XII. It was found from these runs that the smectic phase was stable up to the pressure at which it spontaneously transforms into an isotropic fluid. In Fig. 9 the results from the compression and expansion runs are shown. It can be seen there is no agreement between the results of the compression (starting from an isotropic configuration) and those of the runs which were seeded from a smectic configuration. This is not just a hysteresis loop. The discrepancy arises because the ordered phase obtained by compression and the ordered phase from the expansion runs are different. In fact a nematic phase is obtained by compression whereas in the expansion runs the ordered phase is a smectic one. For a certain density the pressure of the smectic phase is lower than that of the nematic phase. That suggests that the smectic phase can indeed be more stable than the nematic phase for the 9+6 model. The results of this work strongly suggest that the nematic phase does not appear for the 9+6 model. Instead we suggest that a direct isotropic-smectic transition may oc-

TABLE XI. Equation of state for the 9+6 model from NpT MC simulations (compression runs). The notation is as in Tables II and VI.

p^*	y	Z	S_2	$\langle R^2\rangle^{1/2}$	Phase
1.35	0.377	22.65	0.11	6.3759	*I*
1.40	0.381	23.25	0.15	6.3334	*I*
1.45	0.387	23.72	0.22	6.3589	*I*
1.50	0.390	24.33	0.21	6.3864	*I*
1.55	0.396	23.76	0.27	6.3705	*I*
1.60	0.402	25.17	0.29	6.4489	*I*
1.65	0.407	25.65	0.37	6.4744	*I*
1.70	0.409	26.28	0.24	6.4670	*I*
1.75	0.414	26.76	0.28	6.4412	*I*
1.80	0.413	27.60	0.18	6.4146	*I*
1.85	0.415	28.20	0.32	6.4593	*I*
1.90	0.417	28.82	0.15	6.4337	*I*
1.95	0.423	29.14	0.18	6.4038	*I*
2.00	0.422	30.03	0.17	6.4810	*I*
2.05	0.428	30.29	0.33	6.4626	*I*
2.10	0.435	30.56	0.48	6.4801	*N*
2.15	0.440	30.93	0.45	6.5273	*N*
2.20	0.443	31.46	0.43	6.5717	*N*
2.25	0.449	31.71	0.63	6.5663	*N*

TABLE XII. Equation of state for the 9+6 model from NpT MC simulations (expansion and compression runs seeded from a smectic configuration). The notation is as in Tables II and VI. The line dividing the results in the Table divides the compression from the expansion runs.

p^*	y	Z	S_2	$\langle R^2\rangle^{1/2}$	Phase
1.75	0.423	26.17	0.65	6.6935	Sm
1.80	0.431	26.46	0.66	6.7552	Sm
1.85	0.429	27.29	0.62	6.6516	Sm
1.90	0.435	27.66	0.70	6.6542	Sm
1.95	0.438	28.19	0.73	6.7567	Sm
2.00	0.446	28.39	0.70	6.7417	Sm
2.05	0.445	29.15	0.65	6.7371	Sm
2.10	0.447	29.72	0.62	6.6853	Sm
2.15	0.453	30.04	0.73	6.7576	Sm
2.20	0.454	30.70	0.67	6.6961	Sm
2.25	0.456	31.20	0.68	6.7302	Sm
2.30	0.458	31.75	0.68	6.7052	Sm

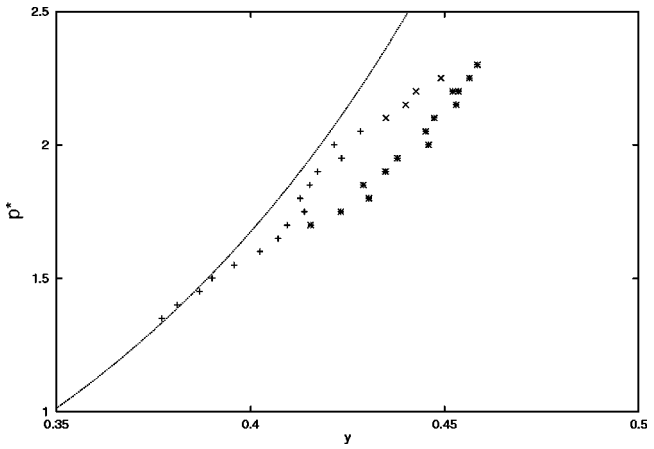

FIG. 9. Equation of state for the 9+6 model. +, 9+6 (isotropic, compression run); ×, 9+6 (nematic, compression run); *, 9+6 (smectic, expansion run from smectic seed configuration). The dotted curve represents the TPT1 EOS for the 15+0 RFFFHS model using the Zhou *et al.* correction.

cur, the nematic phase being completely destabilized for this model.

Let us finish by presenting the global results obtained for models with 15 monomer units. This is done in Fig. 10 where the results for the 15+0, 13+2, 11+4, 10+5, 9+6, and 8+7 are given. This figure illustrates quite clearly the main findings of this work. The EOS of the isotropic fluid is well described by Wertheim's TPT1 and seems to be insensitive to the presence or absence of molecular flexibility. However, the phase diagram is dramatically affected by the presence or absence of flexibility in the tail monomers of the model. Introducing flexibility moves the isotropic-nematic

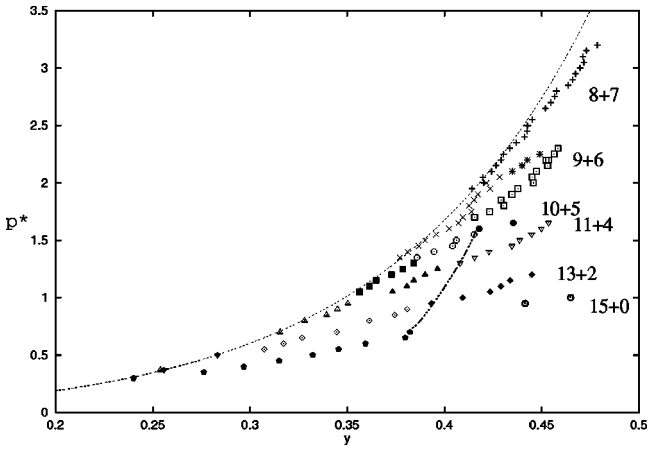

FIG. 10. The equation of state from the MC simulations. +, 8+7 (isotropic); ×, 9+6 (isotropic); *, 9+6 (nematic); □, 9+6 (smectic); ■, 10+5 (isotropic); ⊙, 10+5 (nematic); ●, 10+5 (smectic); △, 11+4 (isotropic); ▲, 11+4 (nematic); ∇, 11+4 (smectic); ▼, 13+2 (isotropic); ◇, 13+2 (nematic); ◆, 13+2 (smectic); solid black pentagon 15+0 (nematic), and the 15+0 (smectic) is a bold open circle. The dotted curve represents the TPT1 EOS for the 15+0 RFFFHS model using the Zhou *et al.* correction. The dot-dashed line is a sketch of the nematic-smectic transition boundary.

transition to higher densities. If the tail is long enough, as in the 8+7 model, then no liquid crystal phase is found at all, also the introduction of the flexible tail makes the nematic phase less stable with respect to the smectic phase. Therefore, we found here a narrow range for the nematic phase for the 11+4 and 10+5 models. For the 9+6 the results of this work suggest a direct transition from the isotropic to the smectic phase. Two phases win and one phase loses when introducing short flexible tails into a rigid model. Isotropic and smectic phases gain further stability by the introduction of flexibility whereas the nematic phase becomes less stable with respect to the other two. However, if the flexible tail is too long, then the smectic phase also looses stability with respect to the isotropic and the only expected transition is the isotropic-ordered solid transition.

V. CONCLUSION

In this paper the effect of flexible tails on the isotropic-nematic transition of hard systems has been analyzed by means of Monte Carlo simulations. The model is formed by m hard spheres with reduced bond length $L^*=0.6$. The first m_r monomers of the chain are rigid and adopt a linear configuration whereas the last m_f monomers are flexible. The model presents symmetry since the rigid core and the flexible tails are formed by the same type of atoms. This feature makes the RFFFHS model suitable for theoretical studies. Three problems have been addressed in this work. First, the phase transitions for two fully rigid models, the 11+0 and the 15+0, have been studied. Second, the effect of adding a flexible tail of four monomer units to the 11+0 model was analyzed. Third, the effect of introducing flexibility in a model of 15 monomers has been studied. For each of these models we have studied the EOS in the isotropic phase, the virial coefficients, and the location of the isotropic-nematic transition. Some preliminary results on the nematic-smectic transition are also reported.

In our view the main conclusions that can be drawn from this work can be summarized as follows.

(i) The virial coefficients are strongly affected by the presence or absence of flexibility in the molecule. The second virial coefficient decreases as the molecule becomes more flexible whereas the opposite behavior is found for the third, and especially for the fourth, virial coefficients.

(ii) The extension of Wertheim's TPT1 EOS proposed by Zhou *et al.* [38] incorrectly describes the low density behavior of the models considered in this work. However, this EOS performs quite well in the medium density region of the isotropic phase. The simulation results of this work illustrate how flexibility hardly affects the equation of state in the isotropic phase of these models at medium densities in agreement with the predictions of TPT1.

(iii) Flexibility dramatically changes the appearance of the phase diagram of hard models. The flexibility plays a major role in determining the location of the liquid crystal phases.

(iv) Fully rigid linear models with 11 or 15 monomer units form nematic and smectic phases. The density of the isotropic-nematic transition moves to lower densities as the

chain becomes more anisotropic.

(v) Adding a flexible tail to a rigid model of 11 monomers shifts the isotropic-nematic transition to much higher pressures and densities. Therefore the addition of tails make the nematic phase much less stable. The configurations adopted by the tail in the isotropic and in the nematic phase are slightly different. In the nematic phase the tails tend to align with the direction of the nematic director.

(vi) Introducing flexibility in a model of 15 monomer units shifts the location of the isotropic-nematic transition to higher densities and pressures. In addition to that our results suggest that smectic phases become more stable by the introduction of flexible tails. Therefore the range of stability of the nematic phase shrinks when flexibility is introduced in the model.

(vii) When the number of monomer units of the flexible tail is too large then no liquid crystal phase is found at all. Too much flexibility prevents the formation of liquid crystal phases.

Since the model used in this work is relatively simple, and taking into account the good description of the EOS of the isotropic phase provided by TPT1 we believe that a theoretical description of the transitions found in this work is possible. We indeed hope that the results of this paper encourage further theoretical work in the area. In addition to this the model can be easily modified to allow for two flexible tails (one at each extreme of the molecule) or even for studying liquid crystal formation in polymer systems (by alternating flexible and rigid sections in a long chain).

To complete the phase diagram of the models presented in this work further work is needed. This is especially true for the solid phases (which were not considered in this work) and for the smectic phases. Our results concerning smectic phases are at this point preliminary due to the small size of the system. Concerning the solid it is relatively simple to generate the close packing structure of the models of this work, taking as a reference the close packed structure of hard dumbbells [51,52]. The study of solid phases would certainly require nonisotropic NpT simulations. For studying in more detail the smectic phase, besides nonisotropic NpT simulations, larger systems and defect free initial configurations are required. We plan to study these transitions in a future work.

Models composed of chains formed from hard spheres (either tangent or overlapping) have become quite popular in the study of flexible molecules. This has been so since the seminal work by Wertheim [36] and Chapmann *et al.* [37], and the simulations of Honnell and Hall [24], Dickman [25], and Dickman and Hall [26]. Here we show that this type of model can also be quite interesting in the study of mesophases for models which combine rigid and flexible sections.

We should, however, mention that for more realistic models, such as models that incorporate bond angles and especially torsional potentials, the effect of flexible tails on the isotropic-nematic transition will not be so drastic. Models that include a torsional potential in the flexible tail(s) are much more inclined to form in the all-*trans* configuration [31]. In our simulations it is not unusual to find a tail curled up on its self, whereas this conformation is rarely found in more ''realistic'' simulations.

ACKNOWLEDGMENTS

Financial support is due to project No. PB97-0329 of the Spanish DGICYT (Dirección General de Investigación Científica y Técnica). One of the authors (C.M.) would like to acknowledge and thank the European Union FP5 Program for financial support (No. HPMF-CT-1999-00163). We also wish to thank the ''Centro de Supercomputacion'' of Universidad Complutense de Madrid for a generous allocation of computer time on their SGI Origin 2000.

[1] L. Onsager, Ann. N.Y. Acad. Sci. **51**, 627 (1949).
[2] N. Metropolis, A. W. Rosenbluth, M. N. Rosenbluth, A. H. Teller, and E. Teller, J. Chem. Phys. **21**, 1087 (1953).
[3] D. Frenkel and B. M. Mulder, Mol. Phys. **55**, 1171 (1985).
[4] D. Frenkel, J. Phys. Chem. **92**, 3280 (1988).
[5] G. T. Evans, Mol. Phys. **87**, 239 (1996).
[6] S. C. McGrother, D. C. Williamson, and G. Jackson, J. Chem. Phys. **104**, 6755 (1996).
[7] P. Bolhuis and D. Frenkel, J. Chem. Phys. **106**, 666 (1997).
[8] P. J. Camp and M. P. Allen, J. Chem. Phys. **106**, 6681 (1997).
[9] D. C. Williamson and G. Jackson, J. Chem. Phys. **108**, 10 294 (1998).
[10] C. Vega and S. Lago, J. Chem. Phys. **100**, 6727 (1994).
[11] K. M. Jaffer, S. B. Opps, and D. E. Sullivan, J. Chem. Phys. **110**, 11 630 (1999).
[12] M. Whittle and A. J. Masters, Mol. Phys. **72**, 247 (1991).
[13] M. J. Maeso and J. R. Solana, J. Chem. Phys. **101**, 9864 (1994).
[14] M. P. Allen and M. R. Wilson, J. Comput.-Aided Mol. Des. **3**, 335 (1989).
[15] G. Vroege and H. N. W. Lekkerkerker, Rep. Prog. Phys. **55**, 1241 (1992).
[16] M. P. Allen, G. T. Evans, D. Frenkel, and B. Mulder, Adv. Chem. Phys. **88**, 1 (1993).
[17] K. J. Toyne, *Liquid Crystal Behavior in Relation to Molecular Structure* (Wiley, New York, 1987), Chap. 2.
[18] M. R. Wilson, Mol. Phys. **85**, 193 (1995).
[19] M. R. Wilson and M. P. Allen, Mol. Phys. **80**, 277 (1993).
[20] M. R. Wilson, Mol. Phys. **81**, 675 (1994).
[21] M. Dijkstra and D. Frenkel, Phys. Rev. E **51**, 5891 (1995).
[22] A. Yethiraj and H. Fynewever, Mol. Phys. **93**, 693 (1998).
[23] H. Fynewever and A. Yethiraj, J. Chem. Phys. **108**, 1636 (1998).
[24] K. G. Honnell and C. K. Hall, J. Chem. Phys. **90**, 1841 (1989).
[25] R. Dickman, J. Chem. Phys. **91**, 454 (1989).
[26] R. Dickman and C. K. Hall, J. Chem. Phys. **89**, 3168 (1988).
[27] A. V. Lyulin, M. S. A. Barwani, M. P. Allen, M. R. Wilson, I. Neelov, and N. K. Allsopp, Macromolecules **31**, 4626 (1998).
[28] K. Nicklas, P. Bopp, and J. Brickmann, J. Chem. Phys. **101**, 3157 (1994).

[29] G. L. Penna, D. Catalano, and C. A. Veracini, J. Chem. Phys. **105**, 7097 (1996).
[30] F. Affouard, M. Kroger, and S. Hess, Phys. Rev. E **54**, 5178 (1996).
[31] C. McBride, M. R. Wilson, and J. A. K. Howard, Mol. Phys. **93**, 955 (1998).
[32] C. McBride and M. R. Wilson, Mol. Phys. **97**, 511 (1999).
[33] J. S. Duijneveldt and M. P. Allen, Mol. Phys. **92**, 855 (1997).
[34] M. R. Wilson, J. Chem. Phys. **107**, 8654 (1997).
[35] D. Levesque, M. Mazars, and J. J. Weis, J. Chem. Phys. **103**, 3820 (1995).
[36] M. S. Wertheim, J. Chem. Phys. **87**, 7323 (1987).
[37] W. G. Chapman, G. Jackson, and K. E. Gubbins, Mol. Phys. **65**, 1 (1988).
[38] Y. Zhou, C. K. Hall, and G. Stell, J. Chem. Phys. **103**, 2688 (1995).
[39] T. Boublik, C. Vega, and M. D. Pena, J. Chem. Phys. **93**, 730 (1990).
[40] M. P. Allen and D. J. Tildesley, *Computer Simulation of Liquids* Oxford University Press, Oxford, 1987).
[41] D. Frenkel and B. Smit, *Understanding Molecular Simulation* (Academic, Orlando, 1996).
[42] R. Eppenga and D. Frenkel, Mol. Phys. **52**, 1303 (1984).
[43] M. R. Wilson, J. Mol. Liq. **68**, 23 (1996).
[44] C. Vega, Mol. Phys. **98**, 973 (2000).
[45] S. Varga and I. Szalai, Mol. Phys. **98**, 693 (2000).
[46] T. Boublik and I. Nezbeda, Collect. Czech. Chem. Commun. **51**, 2301 (1986).
[47] C. Vega, J. M. Labaig, L. G. MacDowell, and E. Sanz, J. Chem. Phys. **113**, 10 398 (2000).
[48] P. A. Monson and M. Rigby, Mol. Phys. **35**, 1337 (1978).
[49] M. Rigby, Mol. Phys. **66**, 1261 (1989).
[50] T. Boublik, Mol. Phys. **68**, 191 (1989).
[51] C. Vega, E. P. A. Paras, and P. A. Monson, J. Chem. Phys. **96**, 9060 (1992).
[52] C. Vega, E. P. A. Paras, and P. A. Monson, J. Chem. Phys. **97**, 8543 (1992).